ISSN NO: 1073 - 7774

Volume 15 Issue 08 August 2024

In Vitro and In Vivo Anti-Cancer Activity Assessment, X-ray Single-Crystal Analysis, and Synthesis of Strong Indolyl-Hydrazones as Kinase Inhibitors for Breast Cancer

1 **V. Prathyusha*,** Asso. Professor, DEPT OF PHARMACEUTICS

2. D. Pitchaiah, Asso. Professor, DEPT OF Pharmacology

3. G. Gayathri, Asst. Professor, DEPT OF Pharmacy Practice

4. G. Adinarayana, Asst. Professor, DEPT OF PHARMACEUTICS

5.**Dr.M. SREENIVASULU**, PRINCIPAL, NARAYANA PHARMACY COLLEGE

[1,2,3,4,5] NARAYANA PHARMACY COLLEGE, CHINTHA REDDY PALEM, NELLORE

Abstract: According to statistics from the World Health Organisation (WHO), 2.3 million women worldwide were diagnosed with breast cancer in 2020; 685,000 of these cases ended in death.In the continuous fight against breast cancer, it is critical to investigate innovative approaches as the disease's incidence numbers continue to grow. As a result, ethyl 3-formyl-1H-indole-2-carboxylate 1 was reacted with thiosemicarbazide and semicarbazide to create a variety of novel indolyl-hydrazones.The new hit compounds were obtained by combining HCl, 4-nitrophenylhydrazine, 2-dinitrophenylhydrazine, and 4-amino-5-(1H-indol-2-yl)-1,2,4-triazole-3-thione. By using NMR, elemental analysis, and X-ray single-crystal analysis, these compounds were given chemical structures asthiosemicarbazone3, bis(hydrazinederivative)5, semicarbzone6, Schiff base 8, and the corresponding hydrazones 10 and 12.The compounds' cytotoxicity against breast cancer cells (MCF-7) was examined using the MTT test.In contrast to staurosproine (IC50 = 8.32±0.43µM), cytotoxicity data showed strong IC50 values against MCF-7, particularly compounds 5, 8, and 12, with IC50 values of 2.73±0.14, 4.38±0.23, and 7.03±0.37µM, respectively. Thus, the wound-healing test was used to examine the activities of compounds 5, 8, and 12 in connection to cell migration. With corresponding percentages of wound closure recorded at 48.8%, 60.7%, and 51.8%, the results demonstrated noteworthy wound-healing effectiveness.By looking at the compounds' ability to induce apoptosis, the effect of the hit compounds on proliferation was evaluated. Remarkably, compound 5 significantly increased cell death in MCF-7 cells, showing a noteworthy 39.26% increase compared to the untreated control group, which showed just 1.27% cell death. Additionally, compound 5's mode of action was examined by testing it against kinase receptors. When compared to conventional medications that target these receptors, the findings showed promising efficacy and considerable kinase inhibition, especially against PI3K-α, PI3K-β, PI3K-δ, CDK2, AKT-1, and EGFR. Using an in vivo experiment, compound 5 showed a significant decrease in tumour volume in the concluding phase, going from 106 mm3 in the untreated control to 56.4 mm3. Additionally, it greatly reduced tumour growth by 46.9%. Because they successfully prevent both cell migration and proliferation, the found leads show promise for possible development into future drugs for the treatment of breast cancer in light of these results.

Keywords: indole; hydrazone; MCF7; anticancer; apoptosis; kinase inhibition

1. Introduction

Cancer is the biggest cause of death worldwide, and breast cancer is one of the top causes of death for women.The intricacy of this condition is a major obstacle to medical treatment. Conventional anticancer therapies have the potential to eradicate cancer cells, but they often cause a host of negative side effects that harm healthy organs. Conventional antitumor medications, which block certain chemicals that promote tumour development, often have adverse effects. As a result, researchers are working hard to develop new anticancer medications and create molecules that are specifically suited to treating different kinds of cancer. The goal of this endeavour is to find tailored medicines that may provide less hazardous and more effective therapeutic alternatives [1,2]. Kinases are essential for cellular activity and make up the sixth biggest family of proteins in the human body [3–5].Because they regulate kinase dysregulation linked to a number of illnesses and disorders, such as cancer, inflammatory conditions, and reactions to external stimuli, kinase inhibitors are essential for preserving appropriate cellular functions.These inhibitors successfully prevent their substrates' development by controlling protein kinases, which allows them to regulate the survival and proliferation of cells [6–9]. Kinase inhibitors may target a wide range of particular targets, including EGFR, CDK, AKT, PI3K, and others [10–12]. Researchers have been interested in indole-containing chemicals for a long time, and the area has developed into a lively one. The creation of novel bioactive drugs is made possible by the indole moiety's high affinity for binding to a variety of receptors.Its extensive use in target-based discovery and anticancer drug design is well-established [13–18]. (4-(pyridin-3-yl)pyrimidin-2-yl)amino)1H-indole-2-carbohydrazide N'-Methylene-5-(Hu et al. [19] reported that the moiety exhibited CDK9 inhibitory action for cancer therapeutic treatment.Compound I, one of the illustrative possibilities presented, was evaluated and shown to have promise against CDK9 inhibition.According to Al-Warhi et al., oxindole II exhibited anti-tumor action by targeting the CDK4 inhibitor [20]. Zhao et al. developed, synthesised, and physiologically evaluated N-substituted iso-indigo compounds as cyclin-dependent kinase 2 (CDK2) inhibitors.It was discovered that iso-indigo compound III halted the cell cycle's S-phase [21]. (Fig. 1).

Advanced renal cell carcinoma (RCC) and gastrointestinal stromal tumours (GIST) are treated with sunitinib [22–25].Tyrosine kinase inhibitors like semaxanib are utilised in cancer treatments [26]. The indole-triazolealkylated system (Figure 1) demonstrated notable anti-cancer properties.For instance, 3-(allylsulfanyl)-4-phenyl-5-(1H-indol-2-yl) and 3-benzylsulfanyl-5-(1H-indol-2-yl)-2H-1,2,4-triazole IV shown encouraging antiproliferative efficacy against HEPG-2 and MCF-7 cancer cell lines [27].The anti-proliferative efficacy of 1,2,4-triazole V and its analogues against breast cancer was intriguing [28]; it replaced 3-(triazolo-thiadiazin-3-yl).-indolin-2-one compoundsIndole-triazole hybrid VII and its analogues demonstrated a strong inhibition against vascular endothelial growth factor receptor-2 (VEGFR-2), with possible anti-renal cancer activity [30]. VI also demonstrated dual inhibition activity for c-Met (a receptor tyrosine kinase) and VEGFR2 enzymes, with an effective anti-proliferative potential against different subpanels of the most NCI58 tumour cell lines [29].By inhibiting VEGFR2 tyrosine kinase, alkylatedindolyl-triazole Schiffbases VIII targeted breast cancer [31].

The idea of creating new compounds that combine esters and azomethine groups with an indole scaffold in one molecule is anticipated to provide powerful anticancer medications, building on the results of the previously described investigations. This expectation is based on the chemicals' ability to interact with receptors as both donors and/or acceptors of hydrogen bonds.

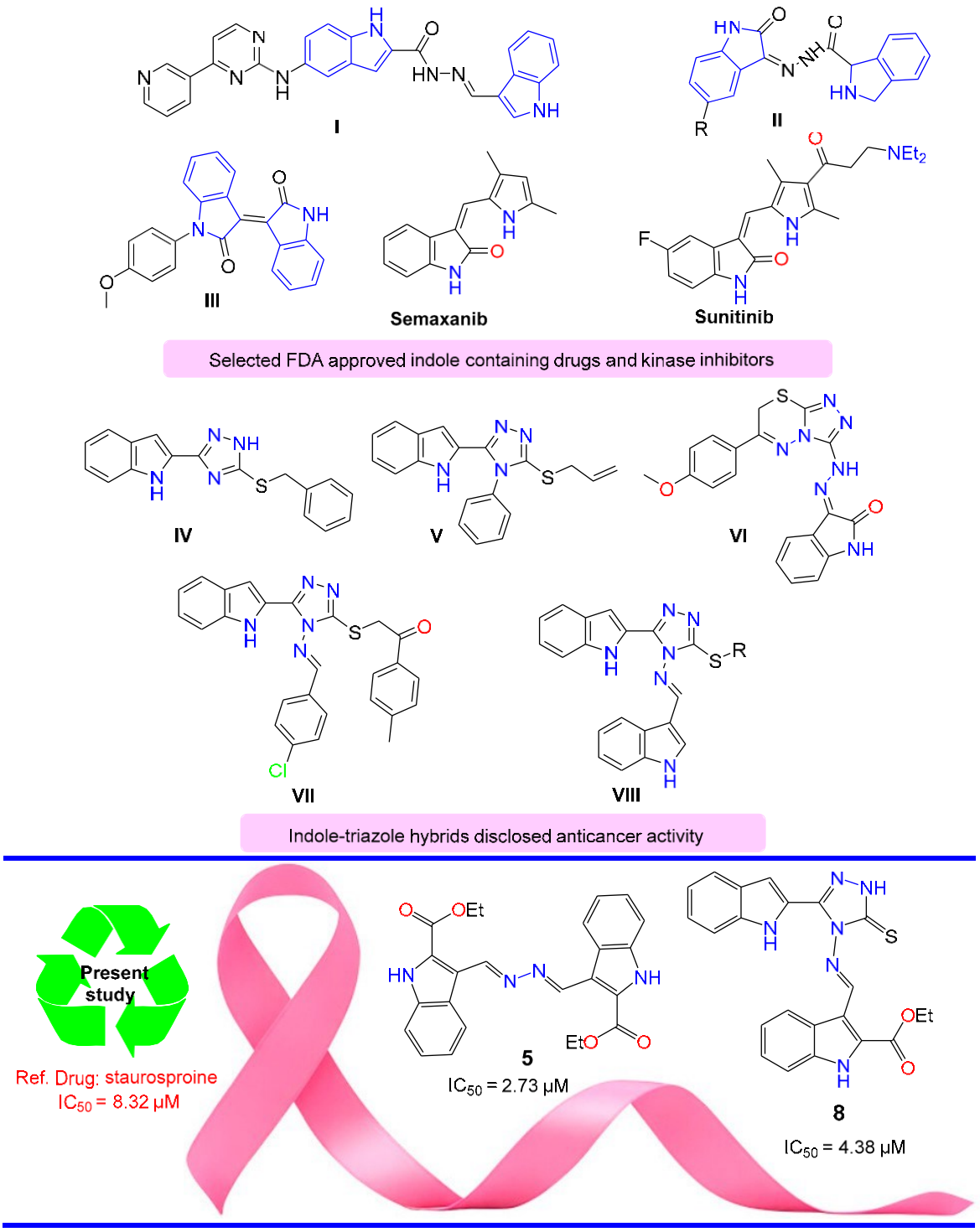

Figure1. Selectedindolestructuresanddrugsthatpossessanticanceractivity.

2. ResultsandDiscussion

Synthesis

Condensation of thiosemicarbazide **2**with ethyl 3-formyl-1*H*-indole-2-carboxylate **1**by fusion for 5 min led to the formation of the thiosemicarbazone derivative **3**.Under the same fusion condition, the condensation of **1**with semicarbazide.HCl **4**interestingly afforded*bis*-esterderivative**5**. Throughthereactionof**1**withsemicarbazide.HCl**4**under reflux in AcOH/MeOH, semicarbazone derivative **6** was obtained (Scheme 1).

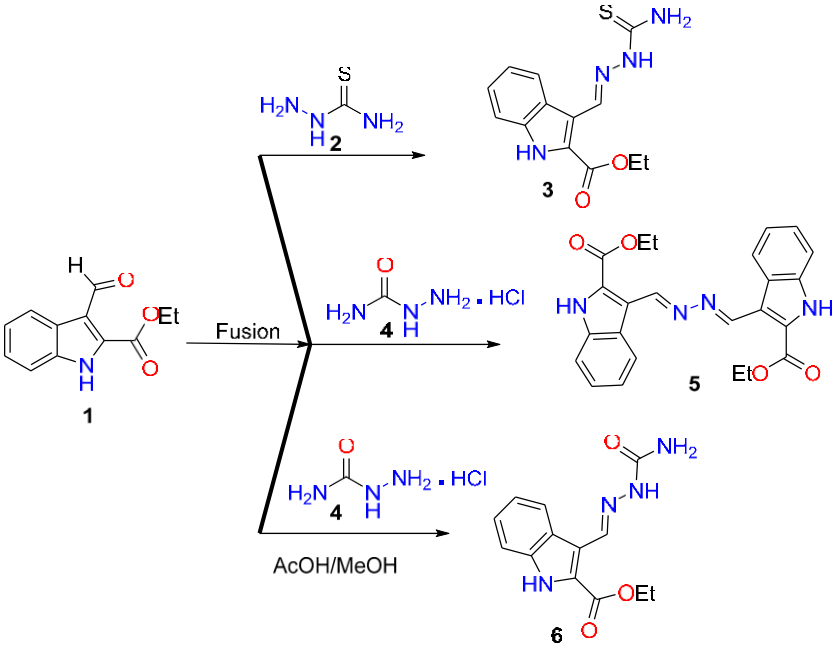

Scheme 1. Reaction of thiosemicarbazide **2** and semicarbazide.HCl **4** with ethyl 3-formyl-1*H*-indole-2-carboxylate **1**.

Under fusion conditions, the reaction between ethyl 3-formyl-1*H*-indole-2-carboxylate **1** with amine functionality derivatives, such as 4-amino-5-(1*H*-indol-2-yl)-1,2,4-triazole-3- thione **7**, 4-nitrophenyl hydrazine **9**,and 2,4-dinitrophenyl hydrazine **11**, resulted in the formationofcondensedhydrazones**8**,**10**,and**12**,respectively(Scheme2). Thestructural assignmentforthenewlysynthesizedhitswasestablishedthroughacomprehensiveset ofspectroscopictools(seeSection3),whichincludednuclearmagneticresonance(NMR), mass spectrometry (MS), CHN analysis, and single-crystal X-ray diffraction analysis.

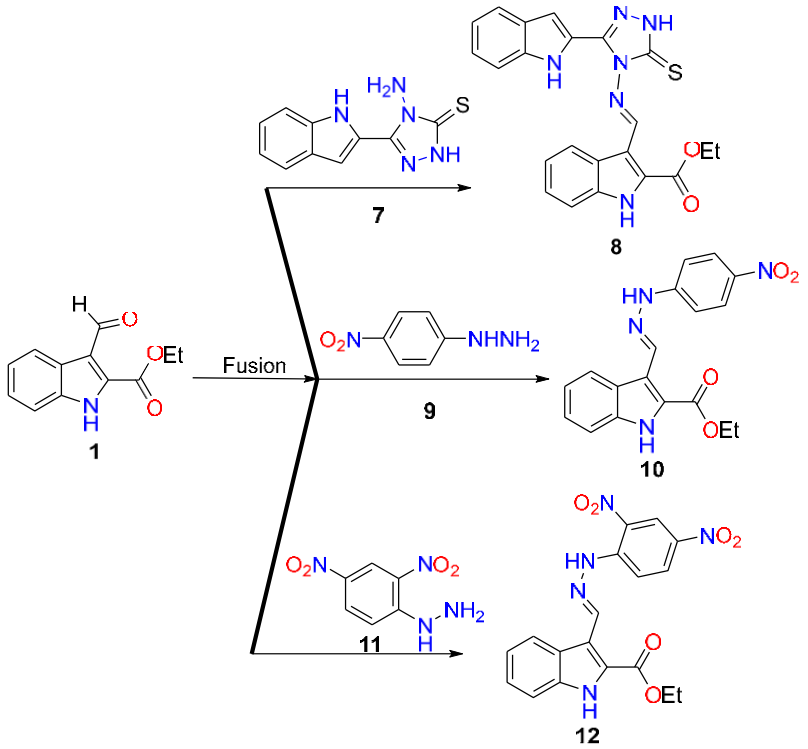

Scheme2. Synthesisofhydrazones**8**,**10**,and**12**.

*X-raySingle-CrystalAnalysisforCompounds***3***and***5**

Using single-crystal X-ray analysis, structures of compounds **3**and **5**were conclusively confirmed.Theunitcellparametersofcompound**3**(*a* =9.23490(10)Å,*b*=19.4168(2)Å,*c* =7.89280(10)Å,and*V*=1374.36(3)Å^3)thatcrystallizedinmonoclinicspacegroup$P2_1/c$ andcompound**5**(*a*=5.4774(3)Å,*b*=9.2031(5)Å,*c*=10.6234(8)(10)Å,and*V*=531.26(6) show the Å^{3}that crystallized in the triclinic space group $P\bar{1}$(Table 1). The crystal structure (Figure 2) revealed that compound **3** was a thiosemicarbazone structure, while compound**5** was a *bis*-hydrazino derivative.

Table1. Crystalsdataofcompounds**3**and**5**.

	3	**5**
CCDC	2293777	2293778
empirical formula	C13H14N4O2S	
	C24H22N4O4fw	290.34
	430.45	
temp(K)	120(2)	120(2)
Λ(Å)	1.54184	0.71073
crystsyst	*Monoclinic*	*Triclinic*
spacegroup	$P2_1/c$	$P\bar{1}$
a(Å)	9.23490(10)	5.4774(3)
b(Å)	19.4168(2)	9.2031(5)
c(Å)	7.89280(10)	10.6234(8)
A(deg)	90	93.995(5)
β(deg)	103.8110(10)	94.008(6)
γ(deg)	90	94.201(5)
V(Å^3)	1374.36(3)	531.26(6)
Z	4	1
ρ_{calc}(Mg/m^3)	1.403	1.345
μ(MoK*α*)(mm^{-1})	2.168	0.094
No.reflns.	16497	8485
Unique reflns.	2884	
	2637Completeness to θ = 67.684°	
	99.8%	
Completenesstoθ=25.242°		99.9%
GOOF(F^2)	1.058	1.046
R_{int}	0.0187	0.0300
$R1^a$($I \geq 2\sigma$)	0.0279	0.0469
$wR2^b$($I \geq 2\sigma$)	0.0780	0.1123

$^a R_1 = \Sigma||F_o|-|F_c||/\Sigma|F_o|$. $^b wR_2 = \{\Sigma[w(F_o^2-F_c^2)^2]/\Sigma[w(F_o^2)^2]\}^{1/2}$.

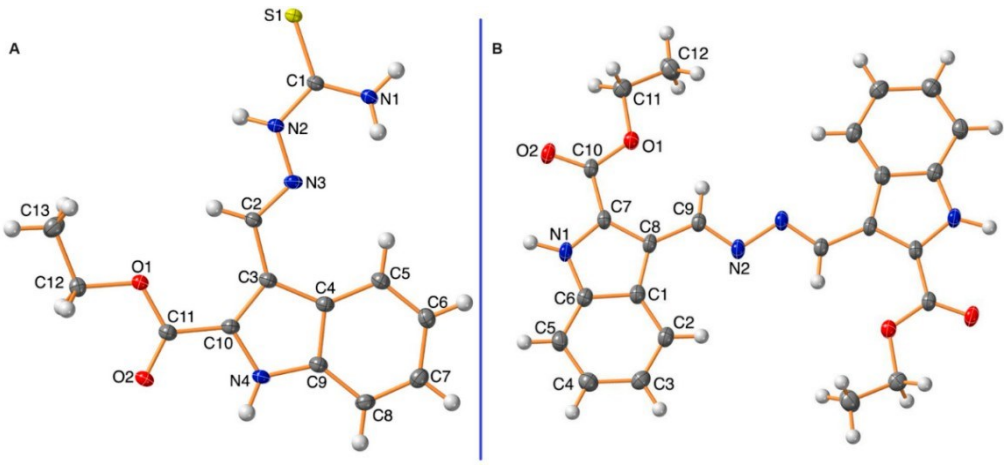

Figure2. Ortepprepresentationof**3**(**A**)and**5** (**B**).

Biology

MTTAssayfortheSynthesized Compounds

The produced compounds were examined for their cytotoxicity against MCF-7 breast cancer cells using the MTT assay.As summarized in Table2, they demonstrated po-tentIC_{50}valuesagainstMCF-7,especiallycompounds**5**,**8**,and**12**,withIC_{50}valuesof 2.73±0.14,4.38±0.23,and7.03±0.37μM,comparedtostaurosproine,withanIC_{50}value of8.32±0.43μM,whilecompounds**1**,**3**,and**6**exhibitedpromisingcytotoxicity,with IC_{50}valuesof 19.7±2.31,10.2±0.53,and 9.42±0.57 μM, respectively.Compound**10** exhibitedmoderatecytotoxicity,withahighconcentrationofIC_{50}(25.4±1.54μM).

Table2. CytotoxicitiesoftheinvestigatedcompoundsagainstMCF-7cellsusingtheMTTassay.

Compounds	IC_{50}±SD[μM]
1	19.7±2.31
3	10.2±0.53
5	2.73±0.14
6	9.42±0.57
8	4.38±0.23
10	25.4±1.54
12	7.03±0.37
Staurosporine	8.32±0.43

IC_{50}valueswere calculatedusing "Mean±SD"of threeindependent values.

Wound-HealingActivity

As shown in Table 3and Figure 3, the wounded area between cell layers following a scratch was partially filled by migrating MCF-7 control cells (94.07% wound closure), while treatments of compounds **5**, **8**, and **12** significantly inhibited wound-healing activity, with percentagesofwoundclosureof48.88,60.74,and51.85%,respectively,comparedtocontrol.

Table3. Thepercentageofwoundhealing(%closure)foruntreatedand**5**-treatedMCF-7cells.

Compound	%Closure*,MCF-7
5	$48.88^{\#}$±2.7
8	$60.74^{\#}$±3.43
12	$51.85^{\#}$±2.92
Untreatedcontrol	94.07±5.5

* Values are expressed as "Mean ±SD". # Significance level (p < 0.05) indicates a significant difference (unpairedStudent'*st*-test)fromtheuntreatedcontrolgroup.Dataforlengthofmigration(mm)andareaaresupportedinthe Supplementary Materials.

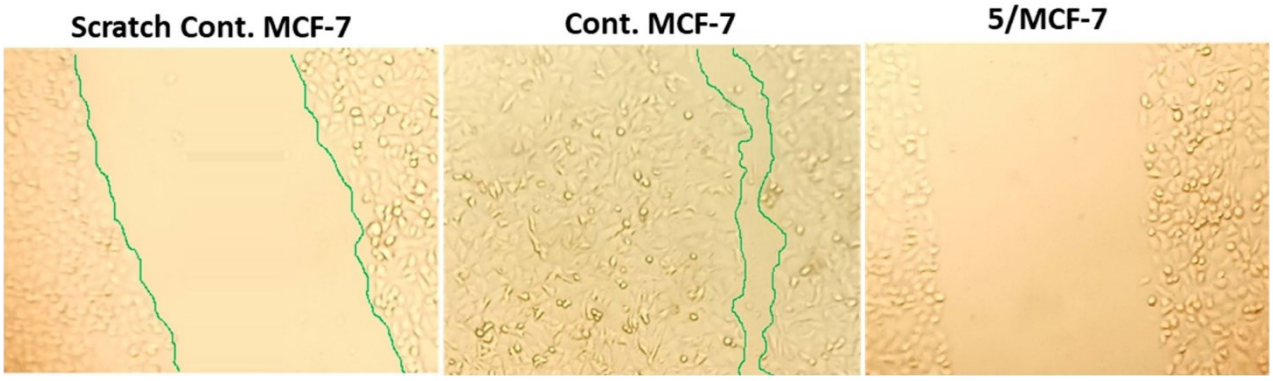

Figure 3. Migration of MCF-7 cells treated with compound **5** for 72 h observed under a lightmicroscope as detected by the wound-healing assay.

ApoptoticInductionActivity

To investigate the apoptotic activity of compounds **5**, **8**, and **12**, flow cytometric evaluation of Annexin V/PI staining was utilized to examine apoptotic cell death inuntreated and treated MCF-7 cells. Table 4shows that compound **5** dramatically increased celldeathinMCF-7cellsby39.26%(29.35%forapoptosisand9.91%fornecrosis),compared to the untreated control group, which increased it by 1.27% (0.4% for apoptosis and 0.87% for necrosis). Additionally, compounds **8** and **12** caused total cell death by 24.4% and 37%, with apoptosis ratios of 15.72% and 21.0%, respectively.

Table 4. Flow cytometry results of the three promising cytotoxic agents using Annexin V/PI and DNA-aided flow cytometry.

Compound	AnnexinV/PIStaining				DNAContent			
	Total	Early	Late	Necrosis	%G0-G1	%S	%G2/M	%Pre-G1
Cont.MCF7	1.27	0.29	0.11	0.87	52.91	41.33	5.76	1.27
5	39.26	7.11	22.24	9.91	39.07	56.19	4.74	39.26
8	24.38	2.27	13.45	8.66	47.10	46.31	6.57	24.38
12	37.05	4.59	17.44	15.02	59.33	38.10	2.55	37.05

After being treated with a cytotoxic chemical, the cell population in each cell phase was then ascertained by DNA flow cytometry.Compound **5** increased the S-phase cell population by 56.2%, compared to control, which increased it by 41.33%, as Figure4illustrates,whereascellsinotherphasesdecreasednegligibly.Consequently,compound**5** stopped MCF-7 cells from proliferating at the S-phase by inducing apoptosis.

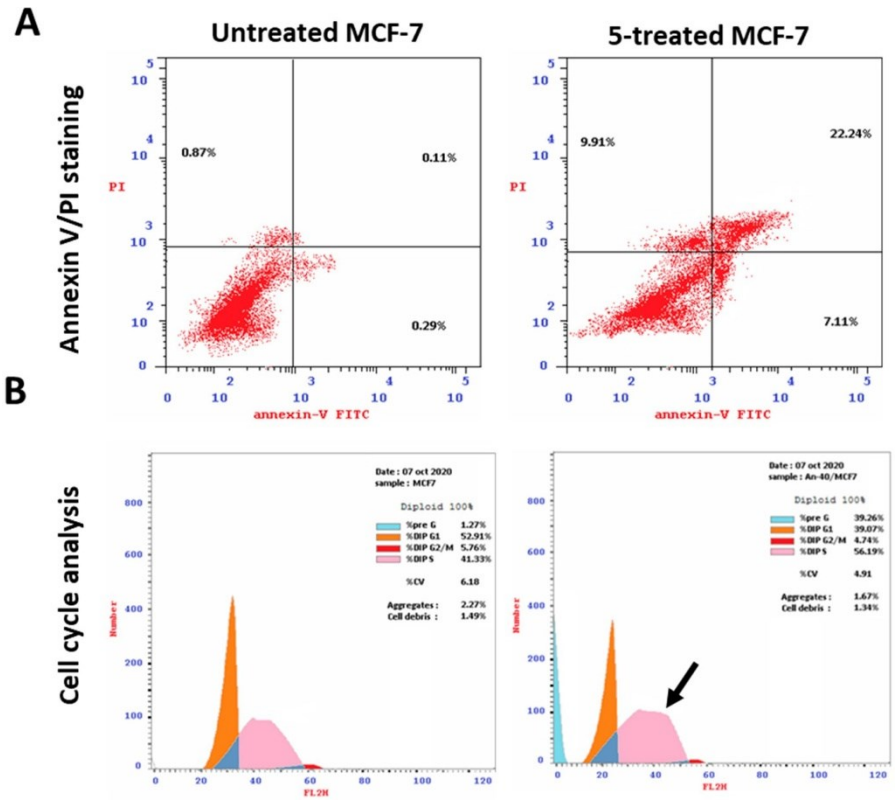

Figure 4. Analysis using flow cytometry.Upper panel (**A**): Annexin V/PI staining for evaluating necrosis and apoptosis, Q1;eEarly apoptosis is Q4, and late apoptosis is Q2.The DNAcontent histogramsofuntreatedand**5**-treatedMCF-7cellsateachphase,"Pre-G,G1,G2/M,S"phases,with an IC_{50} value of 2.73 μM, 48 h, are displayed in the lower panel (**B**).

Kinase-InhibitionActivity

To highlight their effective molecular target, the most cytotoxic and apoptotic com- pound**5**was screened for its activity towards a panel of kinase activities, includingPI3K-*α*,PI3K-*β*,PI3K-*δ*,CDK2,AKT-1,andEGFR,comparedtotheirstandarddrugs. Itcausedpromisingkinaseinhibitoryactivities,assummarizedinTable5. Interestingly, compound **5**exhibited significant inhibitory potential against PI3K-*α*and showed selec- tivity, with a 4.92-fold higher potency than LY294002.However, in the cases of PI3K-*β* and PI3K-*δ*, compound**5**demonstrated lower activity compared to LY294002.More- over, compound**5** (IC_{50} = 0.156±0.01μM) showed a reactivity profile against CDK2 closerto the standard drug erlotinib (IC_{50} of 0.173 ±0.01 μM). On the other hand, com- pound **5** (IC_{50} = 0.602±0.03 μM) demonstrated lower reactivity towards AKT-1, com- pared to the standard drug A-674563 (IC_{50} of 0.26± 0.01μM). Finally, compound**5** (IC_{50}= 0.058±0.029μM) demonstrated lower reactivity against EGFR, compared to thestandarddrugerlotinib(IC_{50}of0.038±0.019μM).Compound**5**wasfoundtopossess the potential for inhibiting multiple kinases.

Table5.IC_{50}valuesofkinaseactivitiesofthetestedcompounds.

Compound	IC_{50}[μM]±SD*					
	PI3K-*α*	PI3K-*β*	PI3K-*δ*	CDK2	AKT-1	EGFR
5	1.73±0.1	2.27±0.11	2.68±0.15	0.156±0.01	0.602±0.03	0.058±0.029
LY294002	8.52±0.48	0.44±0.02	0.85±0.05	NT	NT	NT
erlotinib	NT	NT	NT	0.173±0.01	NT	0.038±0.019
A-674563	NT	NT	NT	NT	0.26±0.01	NT

* "Values are expressed as an average of three independent replicates"."IC_{50} values were calculated using asigmoidal non-linear regression curve fit of percentage inhibition against five concentrations of each compound".NT = Not tested.

InVivo(SEC-BearingMice)

A solid Ehrlich carcinoma cell was implanted, and **5** was injected intraperitoneally (IP) throughout the experiment to confirm its anticancer efficacy, as shown in Figure 5, which summarizes the main findings of the antitumor activity experiments. As a result, tumorproliferationrevealedanincreaseinsolidtumormassofapproximately398.1mg, whichisrelatedtotumorproliferation. Followingtreatmentwith**5**,thesolidtumormass decreasedto126.5mg,comparedto110mginthe5-FUtreatment.Asaresult,treatments with**5**considerablyreducedtumorvolumefrom$10^6$$mm^3$intheuntreatedcontrolto 56.4mm^3andsignificantlydecreasedtumorproliferationby46.9%,while5-FUreduced tumorvolumeto43.7mm^3andinhibitedtumordevelopmentby58.8%.

MolecularDocking

To illustrate the virtual mechanism of binding towards the EGFR, PI3K, and CDK2 bindingsites,moleculardockingresearchwascarriedout. AsseeninFigure6,compound **5**wasproperlydockedinsidetheproteinactivesitesofEGFR(A),PI3K(B),andCDK2(C), with binding energies of −23.15, −21.32, and −23.44 Kcal/mol, and it formed good binding interactions with their active sites. Compound **5** exhibited strong binding interactions with theaminoacidsLys721,Cys773,andLeu694insideEGFR.ItformedtwoH-bondinterac- tionswithVal882insidethePI3Kactivesite,anditformedtwoarene–cationinteractions with Lys89 inside the CDK2 active site like the co-crystallized ligands.These outcomes corroboratedthekinaseinhibitionexperimentfindings. Previousliteraturereportedthe downstream inhibition pathway of EGFR/PI3K/AKT, which is linked to CDK2 inhibition, as a promising target for inducing apoptosis in cancer cells [32].

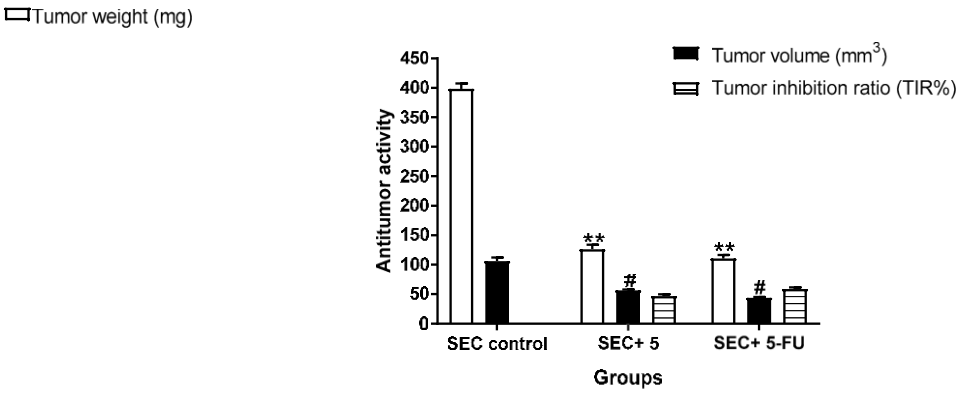

Figure 5. Measurements of antitumor potentiality in the SEC-bearing mice treated with compound **5**and5-FU."Mean±SDvaluesofmiceineachgroup(n =**6**)"."**Valuesarehighlysignificantlydifferent(p≤0.01)between treated and SEC control", while "#values are significantly different (p ≤0.05) betweentreatedSECandSECcontrolmiceusingtheun-pairedtestinGraphPadprism". TIR%=C−T/C×100.

(**A**)

(**B**)

(**C**)

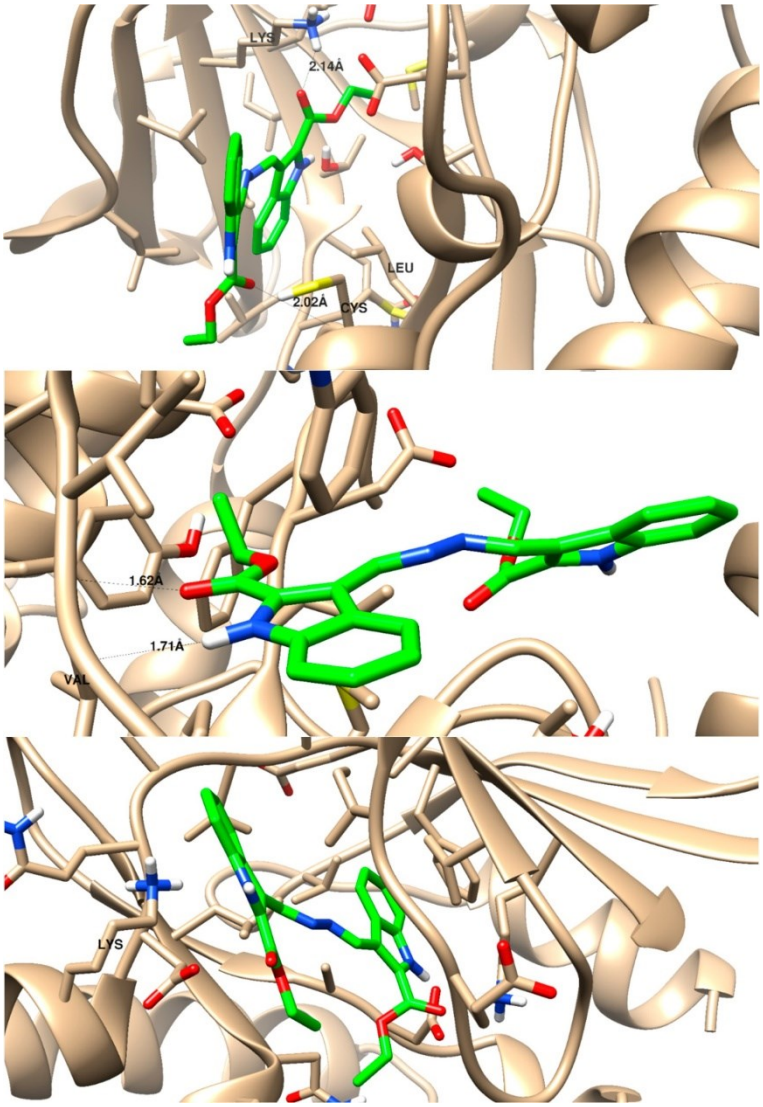

Figure 6. Thebindingdispositionofdockedcompound**5** withligand–receptorinteractionsinsidethe EGFR receptor (**A**), phosphoinositide 3-kinase (**B**), and cyclin-dependent kinase (**C**). Visualizationwas carried out using Chimara-UCSF.

Assummarized inFigure7, compound**5**, as anindolyl-hydrazonederivative, induced potent cytotoxicity against MCF-7 as an apoptosis inducer through the downstreaming pathway of EGFR/PI3K/AKT and CDK2 inhibition. The effective pathway induced cell cycle arrest at the S-phase, and it led to apoptosis in the MCF-7 cells.EGFR, and its downstreamingpathway is considered one ofthe promisingeffective pathwaysfor cancer treatment, and our results agreed with previous reported studies for the same compounds' scaffold affecting cytotoxic activities through apoptosis [33–35].

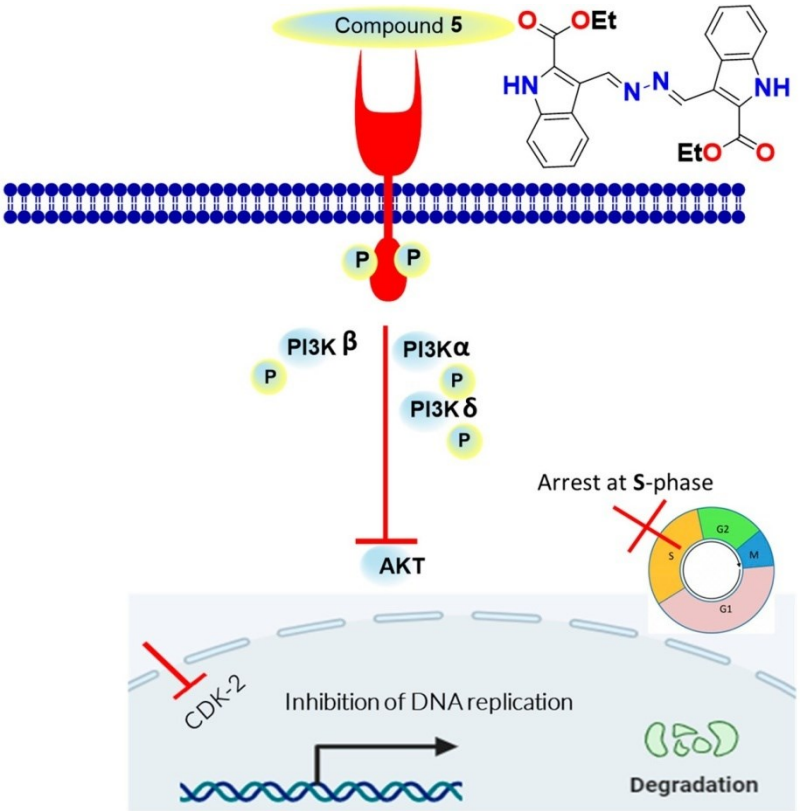

Figure 7. SchematicdiagramforthemechanisticpathwayforEGFR/PI3K/CDK2inhibitionas apoptosis inducers.

SAR

Thestructure–reactivityrelationshipofthesynthesizedcompoundsissummarized as follows in Figure 8: The hydrazone derivative **10**, featuring a *p*-nitro group-substituted benzene ring, exhibited the lowest reactivity, with an IC_{50} value of 25.4 ± 1.54 μM. In contrast, the aldehyde-based indole derivative **1**, the starting material, demonstrated better reactivity, with an IC_{50} value of 19.7 ±2.31 μM. The thiosemicarbazide **3** and its isosteric semicarbazide **6** enhanced reactivity, with IC_{50} values of 9.42 ±0.57 and 10.2 ±0.53 μM, respectively.Thepresenceoftwonitrogroupsonthesubstitutedbenzeneringofhydrazone **12** significantly improved reactivity, with an IC_{50} value of 7.03 ±0.37 μM, due to the high electron-withdrawing group effect. The introduction of the thio-triazole indole-based Schiff base**8** significantlyincreasedactivity(IC_{50}=4.38± 0.23μM)upto1.9-foldhigherthan the reference drug, while the symmetrical *bis*-esters azine **5** emerged as the most potent compound in inhibiting breast cancer cells, with an IC_{50} of 2.73 ± 0.14 μM, 3-fold more potent than the standard drug staurosporine (IC_{50}= 8.32 ± 0.43 μM).

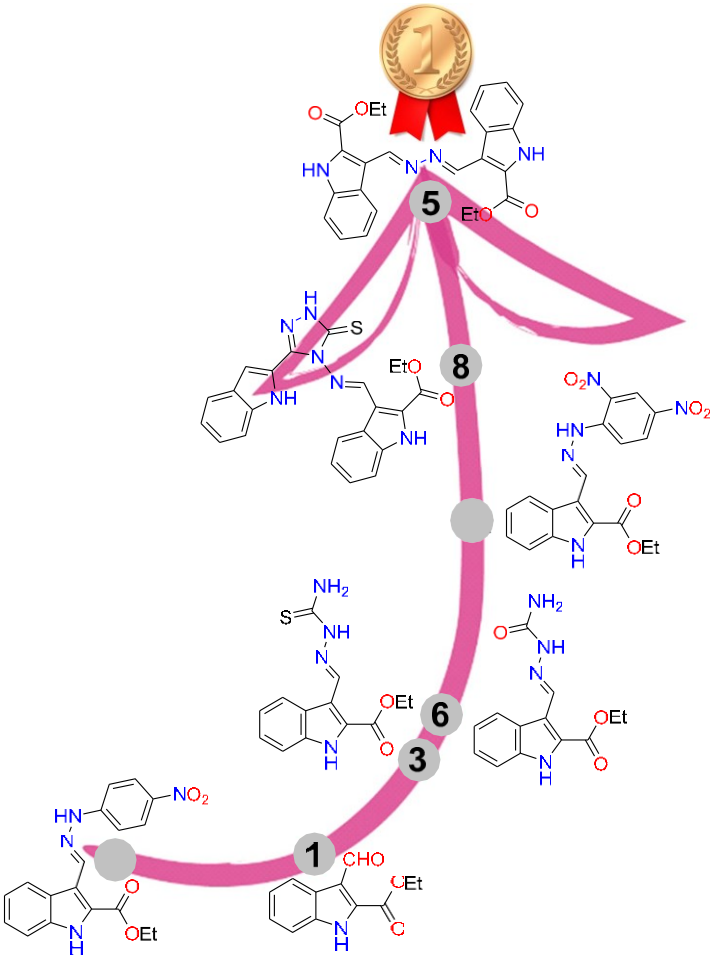

Figure8.SARforthesynthesizedcompounds.

3. MaterialsandMethods

Chemistry

General

The values for the melting points were uncorrected and were determined in open capillaries using a Temp-melt II melting point equipment. On silica gel 60 (230–400 mesh ASTM),flashchromatographywascarriedout.Onsilicagel60F254aluminumplates (E. Merck, layer thickness 0.2 mm), thin-layer chromatography (TLC) was performed. The spotswerefoundusingaUVlamp.UsingDMSO-$d_6$andCDCl_3assolvents,the^{1}Hand ^{13}C-NMRspectrawerecapturedonBrukerinstrumentsat400MHzfor^{1}HNMRand 101 MHz for ^{13}C NMR, respectively. Using KBr and a PerkinElmer 1430 ratio-recording infrared spectrophotometer, Bruker's Fourier-transform infrared (FT-IR) spectrophotometry was used to record the IR spectra.

Synthesis

A mixture of **1** (1.0 mmol, 0.22 g), thiosemicarbazide, and semicarbazide.HCl (1.1 mmol,0.1g,and0.12grespectively)wasgrindedandfusedonahotplatefor5minuntil all reactants turned to products.The products were purified by recrystallization from DMF/EtOH to **3** and **5,** respectively.

Ethyl (*E*)-3-((2-carbamothioylhydrazineylidene)methyl)-1*H*-indole-2-carboxylate **3**. Therewas81%yield,0.23g,andm.p.229–230°C.^{1}HNMR(400MHz,DMSO-d_6):

δ1.41(t,3H,*J*=6.8Hz,CH_3),4.42(q,2H,*J*=6.8Hz,OCH_2),7.21(dd,1H,*J*=7.2,7.6Hz),7.35(dd,1H,*J*=7.2,7.6Hz),7.51(d,1H,*J*=8.0Hz),8.17(brs,2H),8.40(d,1H,*J*=8.4Hz),9.01(s,1H,CH=N-),11.58(s,1H,NH),and12.15(s,1H,NHindole);^{13}CNMR

(100MHz,DMSO-d_6):δ14.69(CH_3),61.60(OCH_2),113.06,115.69,122.32,124.57,124.69,
126.12,127.90,137.04,141.10(9C),161.41(C=O),and177.97(C=S);andelementalanalysis
calculated for [$C_{13}H_{14}N_4O_2S$]:C, 53.78;H, 4.86;N, 19.30;S, 11.04; foundC, 53.89;H, 4.93;
N,19.23;andS,11.09

Diethyl 3,3′-((1*E*,1′*E*)-hydrazine-1,2-diylidene*bis*(methaneylylidene))*bis*(1*H*-indole-2- carboxylate) **5.**

There was 78%yield, 0.34g, andm.p.302–303°C.^{1}H NMR(400 MHz,DMSO-d_6):δ
1.45(t,3H,*J*=6.4Hz,CH_3),4.48(q,2H,*J*=6.4Hz,OCH_2),7.29(dd,1H,*J*=6.8,7.2Hz),
7.41 (dd, 1 H, *J* = 7.2, 6.8 Hz), 7.58 (d, 1 H, *J* = 7.6 Hz), 8.57 (d, 1 H, *J* = 8.0 Hz), 9.59 (s, 1 H, CH=N), and 12.37 (s, 1 H, NH indole); ^{13}C NMR (100 MHz, DMSO-d_6): δ 14.67 (CH_3), 61.70 (OCH_2),113.39,116.09,122.52,124.53,125.34,126.25,128.92,137.07(8C),157.27(C=O),and
161.24(C=O);elementalanalysiscomputedfor[$C_{24}H_{22}N_4O_4$]:C,66.97;H,5.15;N,13.02;
foundC,66.99;H,5.21;andN, 13.13.

Ethyl(*E*)-3-((2-carbamoylhydrazineylidene)methyl)-1*H*-indole-2-carboxylate**6.**

A mixture of **1**(1.0 mmol) and semicarbazide.HCl (1.1 mmol) was refluxed in equal volumesofMeOH/AcOH10mLfor8huntilallreactantsformedproducts. Aprecipitate was formed upon cooling, which was filtered, dried, and recrystallized from MeOH to obtain **6**.

There was 88%yield, 0.25g, andm.p.285–286°C.^{1}H NMR(400 MHz,DMSO-d_6):δ
1.36(t,*J* 7.1Hz,3H),4.37(q,*J*=7.1Hz,2H),6.46(s,2H),7.19(t,*J* =7.5Hz,1H),7.47–7.32
(m,2H),7.55(d,*J*=8.3Hz,1H),7.66(s,1H),8.67(s,1H),and12.31(s,1H,NHindole);
^{13}CNMR(101MHz,DMSO-d_6):δ14.63,61.45,112.10,113.63,121.50,121.95,124.78,125.65,
126.23,134.06,136.85,156.88,and161.24;elementalanalysiscalculatedfor [$C_{13}H_{14}N_4O_3$]:
C,56.93;H,5.15;N,20.43;foundC,57.01;H,5.13;andN,20.52.

Ethyl(*E*)-3-(((3-(1*H*-indol-2-yl)-5-thioxo-1,5-dihydro-4*H*-1,2,4-triazol-4-yl)imino)methyl)- 1*H*-indole-2-carboxylate **8.**

There was 81%yield, 0.36g, andm.p.248–249°C.^{1}H NMR(400 MHz,DMSO-d_6):δ
1.41(t,3H,*J*=6.8Hz,CH_3),4.46(q,2H,*J*=6.8Hz,OCH_2),7.02(dd,1H,*J*=7.2,7.6Hz),
7.20–7.23(m,2H),7.31(dd,1H,and*J*=7.6Hz),7.44–7.52(m,3H),7.65(d,1H,*J*=8Hz),
8.48(d,1H,*J*=8Hz),10.41(s,1H),11.88(s,1H),12.79(s,1H,NHindole),and14.20(brs,1
H,NH_{trz});^{13}CNMR(100MHz,DMSO-d_6):δ 14.60(CH_3),62.17(CH_2),105.59,112.41,113.11,
113.86,120.45,121.55,123.10,123.53,123.86,124.19,125.09,126.61,127.73,131.19,137.12,
137.41, 144.01, 160.84,162.73, and163.31.Calculated elementalanalysis for [$C_{22}H_{18}N_6O_2S$]:
foundC,61.44;H,4.37;N,19.43;S,7.39;C,61.38;H,4.21;N,19.52;O,7.43;andS,7.45

Ethyl(*E*)-3-((2-(4-nitrophenyl)hydrazineylidene)methyl)-1*H*-indole-2-carboxylate**10.**

There was 89%yield, 0.32 g,and m.p.270–271°C.^{1}HNMR (400 MHz,DMSO-d_6):δ
1.43(t,*J*=7.0Hz,3H),4.44(q,*J*=6.9Hz,2H),7.28–7.11(m,2H),7.30(d,*J*=7.4Hz,1H),
7.40(t,*J*=7.6Hz,1H),7.54(d,*J*=8.2Hz,1H),8.18(d,*J*=8.6Hz,2H),8.45(d,*J*=8.1
Hz,1H),8.99(s,1H),11.39(s,1H),and12.13(s,1H,NHindole);^{13}CNMR(101MHz,
DMSO-d_6):δ14.76,61.44,111.43,113.29,117.04,122.20,124.15,124.56,126.23,126.81,137.10,
138.40,139.67,151.01,and161.46;elementalanalysiscalculatedfor[$C_{18}H_{16}N_4O_4$]:C,61.36;
H,4.58;N,15.90;foundC,61.47;H,4.43;andN,15.82.

Ethyl(*E*)-3-((2-(2,4-dinitrophenyl)hydrazineylidene)methyl)-1*H*-indole-2-carboxylate**12.**

There was 89%yield, 0.36g, andm.p.292–293°C.^{1}H NMR(400 MHz,DMSO-d_6):δ
1.44(t,3 H,CH_3),4.46 (q,2H, OCH_2),7.30–7.54(m,3 H), 8.00(brs,1 H),8.38 (brs,2 H),8.83
(brs,1H),9.36(s,1H,CH=N),11.73(s,1H,NH),and12.33(s,1H,NHindole);^{13}CNMR
(100MHz,DMSO-d_6):δ14.72(CH_3),61.67(OCH_2),113.49,115.73,122.76,123.89,126.33,
130.43,137.08,146.62,and161.20;elementalanalysiscalculatedfor[$C_{18}H_{15}N_5O_6$]:C,54.41;
H,3.81;N,17.63;foundC,54.53;H,3.88;andN,17.49.

X-rayStructureDetermination

The general protocol for the collection of crystalline compounds **3**and **5**is provided in the supporting materials [36–38].

4. Cytotoxicity

The breast cancer (MCF-7) cells were obtained and cultivated in RPMI-1640 medium L-glutamine (Lonza Verviers SPRL, Verviers, Belgium, cat#12-604F) using a donation from the National Research Institute in Egypt.Each of the two cell lines was injected with 10% foetal bovine serum (FBS; Sigma-Aldrich, St. Louis, MO, USA) and 1% penicillin-streptomycin (Lonza, Belgium). Following standard tissue culture procedures, all cells were cultivated at 37 °C in 5% CO2 humidified. On the second day of culture, cells were exposed to substances at concentrations of 0.01, 0.1, 1, 10, and 100 µM.The MTT solution (Promega, Madison, WI, USA) was used to assess cell viability after 48 hours [38].After adding 20 µL of MTT dye to each well, the plate was incubated for three hours.After that, absorbance was measured at 570 nm using the ELISA microplate reader (BIO-RAD, modeliMark, Tokyo, Japan). The percentage of cell viability was computed as (mean absorbance of tested compound)/(mean absorbance incontrol)×100, in comparison to the control. Lastly, the nonlinear dose–response sigmoidal curve in GraphPad Prism 7 was used to get the IC50 values [39].Examination of Apoptosis Analysis of the cell cycle and Annexin V/PI staining Six-well culture plates were filled with 3–105 MCF-7 cells, and the plates were left in the incubator overnight.After that, cells were exposed to compound 5 at its IC50 values for 48 hours.The cells and medium supernatants were then collected after PBS had been washed with ice-cold water.The cells were suspended in 100 L of annexin-binding buffer solution, which was made up of 25 mM CaCl2, 1.4 M NaCl, and 0.1 M Hepes/NaOH, pH 7.4, and then treated with "AnnexinV-FITCsolution(1:100)andpropidiumiodide(PI)" at a concentration of 10 g/mL for 30 minutes in the dark. The Cytoflex FACS system was then used to gather labelled cells.The cytExpert tool was used to evaluate the data [39].ScratchAssay's Wound-Healing Assay Previous research mentioned the wound-healing test [40, 41].Four 105 MCF-7 cells were added to six-well plates with starvation medium, and the plates were then incubated for the whole night at 37 °C. Once it was determined the next day that the cells had adhered to the well and that cell confluence had reached 90%, a sterile 1 mL pipette tip was used to agitate a scratch-chop of the cell monolayer. Before the cells were taken off the plates, they were cleaned using starvation medium.The cells with the IC50 of compounds 5, 8, and 12 in the complete medium were cultured for 48 hours in a CO2 incubator.The medium was switched to PBS right away after 48

hours, the wound gap was inspected, and both control and treated cells were photographed using a digital camera that was connected to an Olympus microscope. Measurements were made of the area where the wound closes [42, 43].As directed by the manufacturer, an ELISA kit was used to perform kinase inhibitory assays for EGFR (catalogue #40321), CDK2 (catalogue #79599), AKT (catalogue #78038), PI3K-α (catalogue #40639), β (catalogue #79802), and δ (catalogue #40628). Kinase inhibitory experiments were performed to evaluate compound 5's inhibitory efficacy against the kinase activity. The percentage that chemicals inhibited autophosphorylation was calculated using the formula 100− [(AControl)/(ATreated)− AControl].The IC50 was computed using the percentage inhibition curves of five different chemical doses using the GraphPad Prism7 tool [44].The experimental approach was approved by the Suez Canal University Research Ethics Committee in InVivo (SEC-Bearing Model) (permission number REC219/2023, Faculty of Science, Suez Canal University) [45,46]. The Supplementary Materials provide support for the whole, comprehensive approach.Molecular Docking Maestrow is used to build, optimise, and favour structures in an energetic manner. Following normal work, the AutoDock Vina 1.2.0 program was used to do a molecular docking analysis on the X-ray crystallographic structures of EGFR kinase (PDB ID: 1M17), PI3K (PDB = 1E7V), and CDK2 (PDB = 2A4L) [47,48]. The Chimera-UCSF 1.17.3 software was then used.

5. Conclusions

In order to find new bioactive lead compounds, ethyl3-formyl-1H-indole-2-carboxylate1 acts as a precursor in a series of condensation processes conducted under fusion circumstances. We achieved structure assignments using NMR and X-ray single-crystal analysis. Most of the substances that were synthesised had significant anti-breast cancer properties.When compared to the usual medication, compounds 5, 8, and 12 shown greater activity. With IC50 values of 2.73 ± 0.14 μM, compound 5 showed strong cytotoxicity, three times more effective than staurosporine (IC50 = 8.32 ± 0.43 μM). With a 48.8% wound-closure rate, it also demonstrated strong wound-healing activity. In contrast to their respective conventional medications, compound 5 significantly boosted cell death by apoptosis induction by inhibiting PI3K-α, PI3K-β, PI3K-δ, CDK2, AKT-1, and EGFRkinases. As a result, it is advised that the recently discovered lead molecule be developed further as an anti-breast cancer treatment that targets kinases.

References

1. Ye,F.;Dewanjee,S.;Li,Y.;Jha,N.K.;Chen,Z.-S.;Kumar,A.;Vishakha;Behl,T.;Jha,S.K.;Tang,H.Advancementsinclinical aspectsoftargetedtherapyandimmunotherapyinbreastcancer. *Mol.Cancer***2023**,*22*,105. [CrossRef][PubMed]
2. Senapati,S.;Mahanta,A.K.;Kumar,S.;Maiti,P.Controlleddrugdeliveryvehiclesforcancertreatmentandtheirperformance. *SignalTransduct.Target.Ther.***2018**,*3*, 7.[CrossRef] [PubMed]
3. Ward,R.A.;Goldberg,F.W.*IntroductiontoKinaseDrugDiscovery:ModernApproaches*;RoyalSocietyofChemistry: London,UK, 2018; Volume 67.
4. Zhao,Z.;Bourne,P.E.Progresswithcovalentsmall-moleculekinaseinhibitors.*DrugDiscov.Today***2018**,*23*,727–735.[CrossRef]
5. Bhanumathy, K.K.; Balagopal, A.; Vizeacoumar, F.S.; Vizeacoumar, F.J.; Freywald, A.; Giambra, V. Protein Tyrosine Kinases:Theirroles and their targeting in leukemia. *Cancers***2021**, *13*, 184. [CrossRef]
6. Patterson, H.; Nibbs, R.; McInnes, I.; Siebert, S. Protein kinase inhibitors in the treatment of inflammatory and autoimmunediseases. *Clin. Exp. Immunol.* **2014**, *176*, 1–10. [CrossRef]
7. Bhullar,K.S.;Lagarón,N.O.;McGowan,E.M.;Parmar,I.;Jha,A.;Hubbard,B.P.;Rupasinghe,H.P.V.Kinase-targetedcancer therapies: Progress,challengesandfuturedirections. *Mol. Cancer***2018**,*17*,48. [CrossRef]
8. Bononi,A.;Agnoletto,C.;DeMarchi,E.;Marchi,S.;Patergnani,S.;Bonora,M.;Giorgi,C.;Missiroli,S.;Poletti,F.;Rimessi,A.; etal. Proteinkinasesandphosphatasesinthecontrolofcellfate. *Enzym.Res.***2011**,*2011*,329098. [CrossRef]
9. Valdespino-Gómez,V.M.;Valdespino-Castillo, P.M.;Valdespino-Castillo, V.E. Cell signaling pathways interaction in cellularproliferation:Potentialtargetfortherapeuticinterventionism.*CirugíaCir.***2015**,*83*,165–174.[CrossRef][PubMed]
10. Zhong, L.; Li, Y.; Xiong, L.; Wang, W.; Wu, M.; Yuan, T.; Yang, W.; Tian, C.; Miao, Z.; Wang, T.; et al.Small molecules in targeted cancertherapy:Advances,challenges,andfutureperspectives.*Signal Transduct.Target.Ther.***2021**,*6*,201.[CrossRef][PubMed]
11. You, K.S.; Yi, Y.W.; Cho, J.; Park, J.S.; Seong, Y.S. Potentiating therapeutic effects of epidermal growth factor receptor inhibition intriple-negative breast cancer. *Pharmaceuticals* **2021**, *14*, 589. [CrossRef] [PubMed]
12. Roskoski,R.,Jr.PropertiesofFDA-approvedsmallmoleculeproteinkinaseinhibitors:A2021update.*Pharmacol.Res.***2021**,*165*, 105463.[CrossRef]
13. Spanò, V.; Barreca, M.; Rocca, R.; Bortolozzi, R.; Bai, R.; Carbone, A.; Raimondi, M.V.; Piccionello, A.P.; Montalbano, A.; Alcaro,S.; et al.Insight on [1,3]thiazolo[4,5-e]isoindoles as tubulin polymerization inhibitors.*Eur. J.Med. Chem.***2021**, *212*, 113122. [CrossRef] [PubMed]
14. Ostacolo, C.; Di Sarno, V.; Lauro, G.; Pepe, G.; Musella, S.; Ciaglia, T.; Vestuto, V.; Autore, G.; Bifulco, G.; Marzocco, S.; et al. Identification of an indol-based multi-target kinase inhibitor through phenotype screening and tar-get fishing using inverse virtualscreeningapproach. *Eur. J.Med. Chem.* **2019**,*167*,61–75. [CrossRef][PubMed]
15. Kryshchyshyn-Dylevych, A.; Radko, L.; Finiuk, N.; Garazd, M.; Kashchak, N.; Posyniak, A.; Niemczuk, K.; Stoika, R.; Lesyk, R. Synthesis of novel indole-thiazolidinone hybrid structures as promising scaffold with anticancer potential. *Bioorganic Med. Chem.* **2021**, *50*, 116453. [CrossRef] [PubMed]
16. Wang, G.; He, M.; Liu, W.; Fan, M.; Li, Y.; Peng, Z.Design, synthesisandbiologicalevaluationofnovel2-phenyl-4,5,6,7-tetrahydro- 1H- indole derivatives as potential anticancer agents and tubulin polymerization inhibitors.*Arab. J.Chem.***2022**, *15*, 103504. [CrossRef]
17. Ponnam, D.; Arigari, N.K.; Kalvagunta Venkata Naga, S.S.; Jonnala, K.K.; Singh, S.; Meena, A.; Misra, P.; Luqman, S. Synthesis of non-toxic anticancer active forskolin-indole-triazole conjugates along with their in silico succinate dehydrogenase inhibition studies.*J.Heterocycl.Chem.***2021**,*58*,2090–2101. [CrossRef]
18. Saruengkhanphasit,R.;Butkinaree,C.;Ornnork,N.;Lirdprapamongkol,K.;Niwetmarin,W.;Svasti,J.;Ruchirawat,S.;Eurtivong, C.Identificationofnew3-phenyl-1*H*-indole-2-carbohydrazidederivativesandtheirstructure-activityrelationshipsaspotent tubulininhibitorsandanticanceragents:Acombinedinsilico,invitroandsyntheticstudy.*BioorganicChem.***2021**,*110*,104795. [CrossRef]
19. Hu, H.; Wu, J.; Ao, M.; Zhou, X.; Li, B.; Cui, Z.; Wu, T.; Wang, L.; Xue, Y.; Wu, Z.; et al.Design, synthesis and biological evaluation of methylenehydrazine-1-carboxamide derivatives with (5-((4-(pyridin-3-yl)pyrimidin-2-yl)amino)-1*H*-indole scaffold: NovelpotentialCDK9inhibitors. *BioorganicChem.* **2020**,*102*,104064. [CrossRef]
20. Al-Warhi, T.; El Kerdawy, A.M.; Aljaeed, N.; Ismael, O.E.; Ayyad, R.R.; Eldehna, W.M.; Abdel-Aziz, H.A.; Al-Ansary, G.H.Synthesis, biological evaluation and in silico studies of certain oxindole–indole conjugates as anticancer CDK inhibitors. *Molecules* **2020**, *25*, 2031. [CrossRef]
21. Zhao,P.;Li,Y.;Gao,G.;Wang,S.;Yan,Y.;Zhan,X.;Liu,Z.;Mao,Z.;Chen,S.;Wang,L.Design,synthesisandbiologicalevaluation of N-alkyl or aryl substituted isoindigo derivatives as potential dual Cyclin-Dependent Kinase 2 (CDK2)/Glycogen Synthase Kinase3β(GSK-3β)phosphorylationinhibitors. *Eur.J.Med.Chem.***2014**,*86*,165–174. [CrossRef]
22. Oudard,S.;Beuselinck,B.;Decoene,J.;Albers,P.Sunitinibforthetreatmentofmetastaticrenalcellcarcinoma.*CancerTreat.Rev.* **2011**,*37*,178–184.[CrossRef]
23. Xu, D.; Wang, T.-L.; Sun, L.-P.; You, Q.-D. Recent progress of small molecular VEGFR inhibitors as anticancer agents. *Mini-Rev. Med. Chem.* **2011**, *11*, 18–31. [CrossRef]
24. Gridelli, C.; Maione, P.; Del Gaizo, F.; Colantuoni, G.; Guerriero, C.; Ferrara, C.; Nicolella, D.; Comunale, D.; De Vita, A.; Rossi, A. Sorafenib and Sunitinib

in the Treatment of Advanced Non-Small Cell Lung Cancer.*Oncologist***2007**, *12*, 191–200. [CrossRef] [PubMed]
25. Imming,P.;Sinning,C.;Meyer,A.Drugs,theirtargetsandthenatureandnumberofdrugtargets.*Nat.Rev.DrugDiscov.* **2006**,*5*,821–834.[CrossRef] [PubMed]
26. Lockhart, A.C.; Cropp, G.F.; Berlin, J.D.; Donnelly, E.; Schumaker, R.D.; Schaaf, L.J.; Hande, K.R.; Fleischer, A.C.; Hannah, A.L.; Rothenberg, M.L. Phase I/pilot study of SU5416 (semaxinib) in combination with irinotecan/bolus 5-FU/LV (IFL) in patients withmetastaticcolorectalcancer. *Am.J.Clin.Oncol.***2006**,*29*,109–115. [CrossRef][PubMed]
27. Boraei,A.T.A.;Gomaa,M.S.;ElAshry,E.S.H.;Duerkop,A.Design,selectivealkylationandX-raycrystalstructuredetermination of dihydro-indolyl-1,2,4-triazole-3-thione and its 3-benzylsulfanyl analogue as potent anticancer agents.*Eur. J.Med.Chem.* **2017**, *125*, 360–371. [CrossRef] [PubMed]
28. Boraei, A.T.A.; Singh, P.K.; Sechi, M.; Satta, S. Discovery of novel functionalized 1,2,4-triazoles as PARP-1 inhibitors in breast cancer: Design,synthesisandantitumoractivityevaluation. *Eur.J.Med.Chem.***2019**,*182*,111621. [CrossRef][PubMed]
29. Mohamady, S.; Galal, M.; Eldehna, W.M.; Gutierrez, D.C.; Ibrahim, H.S.; Elmazar, M.M.; Ali, H.I. Dual Targeting of VEGFR2 andC-Met Kinases via the Design and Synthesis of Substituted 3-(Triazolo-thiadiazin-3-yl)indolin-2-one Derivatives as AngiogenesisInhibitors.*ACSOmega***2020**,*5*,18872–18886.[CrossRef]
30. Al-Hussain, S.A.; Farghaly, T.A.; Zaki, M.E.A.; Abdulwahab, H.G.; Al-Qurashi, N.T.; Muhammad, Z.A. Discovery of novel indolyl- 1,2,4-triazole hybrids as potent vascular endothelial growth factor receptor-2 (VEGFR-2) inhibitors with potential anti-renal canceractivity. *BioorganicChem.***2020**,*105*,104330. [CrossRef]
31. Nafie, M.S.; Boraei, A.T.A. Exploration of novel VEGFR2 tyrosine kinase inhibitors via design and synthesis of new alkylated indolyl-triazoleSchiffbasesfortargetingbreastcancer.*Bioorg.Chem.***2022**,*122*,105708.[CrossRef]
32. Lee, D.H.; Szczepanski, M.J.; Lee, Y.J. Magnolol induces apoptosis via inhibiting the EGFR/PI3K/Akt signaling pathway in humanprostatecancercells. *J.Cell.Biochem.***2009**,*106*,1113–1122. [CrossRef][PubMed]
33. Sreenivasulu, R.; Reddy, K.T.; Sujitha, P.; Kumar, C.G.; Raju, R.R. Synthesis, antiproliferative and apoptosis induction potentialactivitiesofnovelbis(indolyl)hydrazide-hydrazonederivatives.*Bioorg.Med.Chem.***2019**,*27*,1043–1055.[CrossRef][PubMed]
34. Das Mukherjee, D.; Kumar, N.M.; Tantak, M.P.; Das, A.; Ganguli, A.; Datta, S.; Kumar, D.; Chakrabarti, G. Development of novel bis(indolyl)-hydrazide–hydrazonederivativesaspotentmicrotubule-targetingcytotoxicagentsagainstA549lungcancercells. *Biochemistry***2016**,*55*,3020–3035. [CrossRef][PubMed]
35. Kilic-Kurt, Z.; Acar, C.; Ergul, M.; Bakar-Ates, F.; Altuntas, T.G. Novel indole hydrazide derivatives:Synthesis and their antiproliferativeactivitiesthroughinducingapoptosisandDNAdamage. *Arch. Pharm.* **2020**,*353*,2000059. [CrossRef]
36. RikaguOxfordDiffraction.*CrysAlisPro*;RikaguOxfordDiffractionInc.:Yarnton,UK,2020.
37. Sheldrick,G.M.SHELXT–Integratedspace-groupandcrystal-structuredetermination.*ActaCryst.***2015**,*A71*,3–8.[CrossRef]
38. Hübschle,C.B.;Sheldrick,G.M.;Dittrich,B.ShelXle:AQtgraphicaluserinterfaceforSHELXL.*J.Appl.Crystallogr.* **2011**,*44*,1281–1284.[CrossRef]
39. VanMeerloo,J.; Kaspers,G.J.L.; Cloos,J.Cell SensitivityAssays:TheMTT Assay.*MethodsMol.Biol.***2011**, *731*,237–245.
40. Mohamed,F.A.M.;Gomaa,H.A.M.;Hendawy,O.M.;Ali,A.T.;Farghaly,H.S.;Gouda,A.M.;Abdelazeem,A.H.;Abdelrahman, M.H.;Trembleau,L.;Youssif,B.G.M.Design,Synthesis,andBiologicalEvaluationofNovelEGFRInhibitorsContaining5-Chloro-3-Hydroxymethyl-Indole-2-Carboxamide Scaffold with Apoptotic Antiproliferative Activity. *Bioorganic Chem.* **2021**, *112*, 104960.[CrossRef]
41. Ali, G.M.E.; Ibrahim, D.A.; Elmetwali, A.M.; Ismail, N.S.M. Design, Synthesis and Biological Evaluation of Certain CDK2 InhibitorsBasedonPyrazoleandPyrazolo[1,5-a]PyrimidineScaffoldwithApoptoticActivity. *BioorganicChem.***2019**,*86*,1–14. [CrossRef]
42. Qin, X.; Han, X.; Hu, L.; Li, Z.; Geng, Z.; Wang, Z.; Zeng, C.; Xiao, X. Design, Synthesis and Biological Evaluation of Quinoxalin- 2(1H)-OneDerivativesasEGFRTyrosineKinaseInhibitors.*Anticancer.AgentsMed.Chem.***2015**,*15*,267–273.[CrossRef]
43. AkgÜl,Ö.;Erdo Ğan,M.A.;BI ̇rI ̇m,D.;KayabaS ̧i,Ç.;GÜndÜz, C.;Arma Ğan, G.Design,Synthesis, CytotoxicActivity,and ApoptosisInducingEffectsof4-andN-SubstitutedBenzoyltaurinamideDerivatives.*Turk.J.Chem.***2020**,*44*,1674–1693.[CrossRef]
44. Turner, D.P.; Moussa, O.; Sauane, M.; Fisher, P.B.; Watson, D.K. Prostate-derived ETS factor is a mediator of metastatic potentialthrough the inhibition of migration and invasion in breast cancer.*Cancer Res.* **2007**, *67*, 1618–1625.[CrossRef]
45. Chen, Y.; Lu, B.; Yang, Q.; Fearns, C.; Yates, J.R.; Lee, J.-D. Combined Integrin Phosphoproteomic Analyses and siRNA-based Functional Screening Identified Key Regulators for Cancer Cell Adhesion and Migration.*Cancer Res.***2009**,*69*, 3713–3720. [CrossRef] [PubMed]
46. Barghash,R.F.;Eldehna,W.M.;Kovalová,M.;Vojáčková,V.;Kryštof,V.;Abdel-Aziz,H.A.One-PotThree-ComponentSynthesis ofNovelPyrazolo[3,4-b]PyridinesasPotentAntileukemicAgents. *Eur. J.Med. Chem.* **2022**,*227*,113952. [CrossRef]
47. Noser,A.A.;Abdelmonsef,A.H.;Salem,M.M.Design,SynthesisandMolecularDockingofNovelSubstitutedAzepinesas InhibitorsofPI3K/Akt/TSC2/mTORSignalingPathwayinColorectalCarcinoma.*Bioorganic Chem.***2023**,*131*,106299.[CrossRef]
48. Lapillo, M.; Tuccinardi, T.; Martinelli, A.; Macchia, M.; Giordano, A.; Poli, G. Extensive Reliability Evaluation of Docking-Based Target-FishingStrategies. *Int. J.Mol. Sci.* **2019**,*20*,1023. [CrossRef][PubMed]
49. Dhanalakshmi, B.; Anil Kumar, B.M.; Srinivasa Murthy, V.; Srinivasa, S.M.; Vivek, H.K.; Sennappan, M.; Rangappa, S. Design, Synthesis and Docking Studies of Novel 4-Aminophenol-1,2,4-Oxadiazole Hybrids as Apoptosis Inducers against Triple Negative Breast Cancer Cells Targeting MAP Kinase. *J.Biomol. Struct. Dyn.* **2023**, 1–17. [CrossRef] [PubMed]
50. Dicato,M.;Plawny,L.;Diederich,M.Anemiaincancer.*Ann.Oncol.***2010**,*21*,vii167–vii172.[CrossRef]
51. HEl Zahabi, S.A.; Nafie, M.S.; Osman, D.; Elghazawy, N.H.; Soliman, D.H.; EL-Helby, A.A.H.; Arafa, R.K. Design, synthesis and evaluation of new quinazolin-4-one derivatives as apoptotic enhancers and autophagy inhibitors with potent antitumor activity.*Eur. J.Med. Chem.* **2021**,*222*,113609.
52. Boraei, A.T.A.; Eltamany, E.H.; Ali, I.A.I.; Gebriel, S.M.; Nafie, M.S. Synthesis of new substituted pyridine derivatives as potent anti-liver cancer agents through apoptosis induction: Invitro, invivo, and in silico integrated approaches.*Bioorganic Chem.* **2021**, *111*, 104877. [CrossRef]